Published in final edited form as:

Mol Carcinog. 2022 October ; 61(10): 958–971. doi:10.1002/mc.23453.

TGFβ1 regulates HRas-mediated activation of IRE1α through the PERK-RPAP2 axis in keratinocytes

Saie Mogre[1], **Nicholas Blazanin**[1,2], **Hailey Walsh**[1], **Jack Ibinson**[1], **Chase Minnich**[1], **Chih-Chi Andrew Hu**[3], **Adam B Glick**[1]

[1]Department of Veterinary and Biomedical Sciences, Pennsylvania State University, University Park, PA 16802

[2]Current Address: Department of Thoracic and Cardio Surgery-Research, The University of Texas M D Anderson Cancer Center, Houston, TX 77054

[3]Center for Translational Research in Hematologic Malignancies, Houston Methodist Cancer Center, Houston Methodist Research Institute, Houston, TX 77030

Abstract

Transforming Growth Factor β1 (TGFβ1) is a critical regulator of tumor progression in response to HRas. Recently, TGFβ1 has been shown to trigger ER stress in many disease models; however, its role in oncogene-induced ER stress is unclear. Oncogenic HRas induces the unfolded protein response (UPR) predominantly via the Inositol-requiring enzyme 1α (IRE1α) pathway to initiate the adaptative responses to ER stress, with importance for both proliferation and senescence. Here, we show a role of the UPR sensor proteins IRE1α and (PKR)-like endoplasmic reticulum kinase (PERK) to mediate the tumor-suppressive roles of TGFβ1 in mouse keratinocytes expressing mutant forms of HRas. TGFβ1 suppressed IRE1α phosphorylation and activation by HRas both in *in vitro* and *in vivo* models while simultaneously activating the PERK pathway. However, the increase in ER stress indicated an uncoupling of ER stress and IRE1α activation by TGFβ1. Pharmacological and genetic approaches demonstrated that TGFβ1-dependent dephosphorylation of IRE1α was mediated by PERK through RNA Polymerase II Associated Protein 2 (RPAP2), a PERK-dependent IRE1α phosphatase. In addition, TGFβ1-mediated growth arrest in oncogenic HRas keratinocytes was partially dependent on PERK-induced IRE1α dephosphorylation and inactivation. Together, these results demonstrate a critical cross-talk between UPR proteins that is important for TGFβ1-mediated tumor suppressive responses.

Keywords

Unfolded Protein Response; ER Stress; IRE1α; PERK; HRas; TGFβ1; Proliferation

Introduction

Inositol-requiring enzyme 1α (IRE1α), Protein kinase RNA-like ER kinase (PERK), and activating transcription factor 6 (ATF6) are the three unfolded protein response (UPR) sensors that mediate adaptation to endoplasmic reticulum (ER) stress caused by the dysregulated proteostasis that is frequently observed in tumor cells[1]. The UPR is an integrated series of signaling pathways that can optimally meet the demands of protein

synthesis to folding under physiological as well as pathological conditions[1,2]. Accumulation of unfolded proteins can activate the UPR sensors either upon its dissociation with Grp78 (or BiP), an ER-resident chaperone, or by direct association with the unfolded proteins in the ER lumen[3,4]. Upon activation, the multi-domain IRE1α can dimerize and subsequently oligomerize via its kinase domain under increasing levels of ER stress by undergoing auto- and transphosphorylation. This causes a conformational change in its RNase domain to recognize *Xbp1* mRNA, its major target[5]. The unconventional splicing of *Xbp1* mRNA removes a 26bp intron to code a transcription factor XBP1S that can regulate the transcription of certain ER chaperones such as DnaJ-like proteins, *Pdi*, *Ero1-Lα*, *Sec61a1*, and *BiP* in addition to genes involved in ER-associated degradation (ERAD) machinery such as *Edem1*[6-10]. In addition, the IRE1α RNase can also selectively recognize and degrade an array of mRNAs and miRNAs of ER-targeted proteins by a process known as regulated IRE1-dependent decay (RIDD)[11,12]. On the contrary, an activated PERK dimer can phosphorylate its downstream effector, eIF2α, leading to the global inhibition of protein translation but can also selectively translate ATF4, a transcription factor that can regulate a diverse set of biological functions during prolonged ER stress[13,14]. Activated ATF6 undergoes proteolytic cleavage by site-1 and site-2 proteases to encode a transcription factor that in turn upregulates expression of *Xbp1*, *BiP*, *Pdi*, and *Edem1*[15,16].

Increased IRE1α and XBP1 expression have been associated with tumor aggressiveness in multiple cancers[17–22]. Constitutive activation of the Ras pathway due to the presence of mutations is estimated in about 19% of all cancer lesions[23]; however, irreversible growth arrest and premature senescence by oncogenic HRas is an initial tumor-suppressive response observed in benign lesions of the skin[24,25]. Previous research from our lab has shown that oncogenic HRas-dependent activation of IRE1α, but not PERK, can govern the paradoxical proliferative and senescence phenotypes frequently observed in primary keratinocytes expressing oncogenic mutants of HRas[26]. XBP1S generated by activated IRE1α is essential for the proliferative response, while RIDD is critical for senescence[26].

Oncogenic HRas also induces secretion of TGFβ1 in primary keratinocytes[27,28], a major regulatory cytokine in normal and transformed epithelial cells[27,29–35]. Interestingly, HRas does not block the early biochemical events of TGFβ1 signaling but leads to global changes in gene expression[36]. TGFβ1 can accelerate premature senescence in v-Ras^{Ha}-expressing keratinocytes and inactivation of TGFβ1 responses or production causes benign tumors to undergo rapid malignant conversion[37,38]. Studies have highlighted the roles of TGFβ1 signaling to modulate the tumor-suppressive or promoting function of oncogenic HRas[28,32] and to induce ER stress in fibrosis[39–42], differentiation[43], inflammation[44], and apoptosis[45]; however, the role of TGFβ1 in regulating oncogene-induced ER stress during early stages of cancer development remains poorly understood. Here, we investigate the ability of TGFβ1 to modulate ER stress in oncogenic HRas-expressing keratinocytes and show its importance in TGFβ1-mediated growth inhibition.

Results

TGFβ1 blocks HRas-induced activation of IRE1α, but does not suppress the ER stress response

We previously showed that expression of oncogenic HRas in primary mouse keratinocytes either through retroviral transduction of oncogenic HRas (v-Ras^{Ha}) or doxycycline induction of an HRas^{G12V} transgene caused a MEK-ERK-dependent increase in total and phosphorylated IRE1α, *Xbp1* splicing, and elevated ER stress[26]. To test the effect of TGFβ1 on HRas-mediated IRE1α activation, we induced HRas^{G12V} in primary K5rTA x tetO-HRas^{G12V} (K5Ras) keratinocytes with increasing doses of doxycycline with and without TGFβ1. As expected, HRas^{G12V} significantly activated IRE1α even at the lowest level of expression (50 ng/ml doxycycline) as determined by elevated total and phosphorylated IRE1α expression detected by Western blot and phos-tag SDS-PAGE, which can reveal total levels of protein phosphorylation, but this increase was blocked by 1 ng/ml TGFβ1 (Figure 1A). Specifically, TGFβ1 diminished the level of HRas-induced IRE1α phosphorylation at ser729, a critical phosphorylation site in the kinase activation loop[46–48], although not to the same extent as the total phosphorylation (Figure S1A). While the TGFβ1-dependent decrease in IRE1α phosphorylation in HRas keratinocytes was accompanied by a marginal reduction in total IRE1α protein (Figure 1A), IRE1α mRNA was not significantly modulated compared to HRas alone (Figure S1B). In addition, there was a significant reduction in HRas-induced *Xbp1* mRNA splicing measured by both qPCR and a *Xbp1* splicing assay, further supporting that TGFβ1 caused inactivation of IRE1α RNase in these cells (Figure 1B, S1C). Consistent with lower *Xbp1s* mRNA, HRas-indued increase in *Ero1-Lα* mRNA, which encodes an ER-resident oxidoreductase important in protein disulphide bond formation[49] was suppressed by TGFβ1 (Figure S1H). Similarly, TGFβ1 suppressed IRE1α phosphorylation and *Xbp1* splicing induced by v-Ras^{Ha} in primary keratinocytes (Figure 1C, S1D, E). Consistent with the decreased IRE1α phosphorylation and spliced *Xbp1* mRNA, TGFβ1 caused lower XBP1S protein and its downstream effector Grp78 or BiP, an ER-resident chaperone (Figure 1A, C, S1E). At the same time, the decrease in IRE1α phosphorylation by TGFβ1 in HRas-expressing keratinocytes was not associated with further changes in mRNA expression of previously validated HRas-dependent RIDD targets *Id1*, *Igfbp2*, *Hgsnat*, *Pmp22*, and *Timp3*[26] (Figure S1F, G) or of ER-stress associated genes, *p58^{IPK}* and *BiP* (Figure S1H). Nonetheless, TGFβ1 caused an increase in the mRNA expression of a HRas-dependent RIDD target, *Adamts1*[26] (Figure S1F), suggesting a possible gene-specific role. Analogous to our *in vitro* observations, we detected significantly reduced levels of IRE1α phosphorylation in DMBA-TPA induced benign epidermal papilloma overexpressing active TGFβ1[50] compared to control papilloma (Figure 1D, E).

Oncogenic HRas causes ER stress in keratinocytes[26]. To determine if suppression of IRE1α signaling by TGFβ1 altered ER stress levels, we used Thioflavin T (ThT), a fluorescent marker of ER stress that detects aggregated proteins in the ER lumen[51]. Surprisingly, TGFβ1 caused a significantly higher accumulation of misfolded proteins in HRas keratinocytes compared to either HRas or TGFβ1 alone (Figure 1F, G, S2A). The increase in fluorescence was blocked in cells pre-treated with 2.5 mM 4-Phenylburyric Acid (4-PBA), a chemical

chaperone that aids in protein folding and prevents aggregation in the ER[26,52], indicating that higher ThT fluorescence was associated with elevated ER stress (Figure S2B, C). In addition, using ER Tracker™ Green, a cell-permeable dye that preferentially detects the K+ channels of the ER, we found that TGFβ1 caused a sustained expansion of the ER both in terms of absolute area and mean fluorescence intensity in control keratinocytes but did not cause a further increase in HRas keratinocytes (Figure 1H-J). Together, these results indicate that the reduction of IRE1α activation by TGFβ1 is not a secondary consequence of reduced ER stress but reflects an uncoupling by TGFβ1 of the HRas-induced IRE1α activation and the ER stress response.

TGFβ1 activates PERK signaling in keratinocytes

While TGFβ1 dampened the IRE1α-dependent UPR response in keratinocytes, it increased PERK signaling as measured by higher total and phosphorylated PERK, phospho-eIF2α and CHOP protein expression after 48h compared to both the control and HRas keratinocytes (Figure 2A, B). However, TGFβ1 alone caused an increase in total and phosphorylated PERK; and increasing levels of HRas did not meaningfully regulate PERK activation as previously shown[26] (Figure 2B, S3A). Similarly, while TGFβ1 increased *Perk*, *Pdia4*, and *Pdia5* mRNA expression (Figure 2C) suggesting TGFβ1-dependent activation of PERK signaling in these keratinocytes[53], no additional effect of HRas on expression of these genes was observed (Figure S3B). Furthermore, Western blot showed higher total PERK, phospho-eIF2α, ATF4, and CHOP expression even at a low dose of 0.25 ng/ml TGFβ1. This activation was blocked in keratinocytes pre-treated with GSK2606414, a PERK inhibitor (PERKi) at a non-cytotoxic dose that can prevent thapsigargin-induced PERK activation (Figure 2D, S3C). In contrast, although IRE1α expression remained unchanged, ATF6 expression decreased with increasing doses of TGFβ1 (Figure 2D). Together, this data demonstrates that PERK signaling is selectively activated by TGFβ1 independent of HRas-induced ER stress in keratinocytes.

TGFβ1-mediated inhibition of IRE1α ER stress response is dependent on PERK

A number of studies have investigated crosstalk between the three UPR sensor proteins under ER stress as a determinant of cell survival[54–57]. To test if TGFβ1-dependent IRE1α dephosphorylation in HRas keratinocytes required PERK activation, we treated primary K5Ras keratinocytes with PERKi with and without TGFβ1. 250 nM PERKi decreased total and phosphorylated PERK levels without modulating IRE1α or BiP expression in control keratinocytes as expected (Figure 3A, S4A). In HRas keratinocytes, phos-tag Western blot for total phosphorylated IRE1α showed a partial reversal of TGFβ1-induced IRE1α dephosphorylation by PERKi. However, no significant reversal was observed at ser729, suggesting changes at other phosphorylation sites were important (Figure S4B). The reversal in total IRE1α phosphorylation was coupled with increased spliced XBP1 and BiP expression in these keratinocytes (Figure 3A, S4A). Interestingly, spliced *Xbp1* mRNA was significantly increased even in PERK-inhibited control keratinocytes treated with TGFβ1, further supporting the importance of PERK in regulating IRE1α phosphorylation and activity by TGFβ1 (Figure S4C). Moreover, treatment with PERKi significantly reduced the level of unfolded proteins measured by ThT fluorescence in TGFβ1-treated HRas keratinocytes (Figure 3B, C), consistent with its ability to partially restore IRE1α activity.

To test this further, we generated an immortalized C57BL/6 keratinocyte cell line (C57-T) expressing a doxycycline-inducible wildtype human IRE1α through lentiviral transduction. These cells were then transduced with the v-Ras^{Ha} retrovirus and treated with TGFβ1 under the conditions of IRE1α overexpression and an associated increase in autophosphorylation (Figure S4D). Figures 3B and 3C show that overexpression of IRE1α significantly reduced the intensity of ThT fluorescence in TGFβ1-treated v-Ras^{Ha} keratinocytes compared to the control, supporting the idea that restoration of IRE1α activity by PERKi can lower the ER burden of unfolded proteins. Together, these results demonstrate that IRE1α is the critical UPR pathway for dampening HRas-induced ER stress and that activation of the PERK arm of the UPR by TGFβ1 both inhibits IRE1α phosphorylation and the ER stress response.

TGFβ1 mediated growth arrest is dependent on modulation of IRE1α and PERK

Previous studies have shown a direct role of the IRE1α pathway to promote proliferation while inactivation can also contribute to tumor progression[26,58,59]. On the contrary, we have shown a role for IRE1α in HRas-induced senescence, a mechanism of tumor suppression[26]. Elevated ER stress is also associated with reduced survival[60–62]. Using an MTT assay to measure the number of surviving cells in TGFβ1-treated HRas keratinocytes, we observed a significant reduction in survival in TGFβ1-treated control keratinocytes, and a greater decrease in HRas keratinocytes (Figure 4A). Additionally, as expected, mutant HRas^{G12V} increased cell proliferation measured by percent BrdU positive cells while TGFβ1 suppressed proliferation in control, HRas^{G12V} or v-Ras^{Ha}-transduced keratinocytes (Figure 4B, S5A-C) and this was consistent with a significant increase in cell numbers at 96h as well as an increase in the numbers of colonies formed by the K5Ras-T keratinocytes expressing mutant HRas^{G12V} compared to its control and a significant decrease in colony formation both in terms of their relative size and number when treated with 1 ng/ml TGFβ1 (Figure S5G-I). In contrast, TGFβ1 did not alter either the percent of early (Annexin V positive) or late (Annexin V and PI positive) apoptotic populations in HRas keratinocytes compared to the untreated controls after 48h (Figure S5D-F). Collectively, these data suggest reduced proliferation in TGFβ1-treated HRas keratinocytes was responsible for the reduced cell viability measurement.

To determine if IRE1α dephosphorylation by the TGFβ1-PERK axis was required for the effects of TGFβ1 on cell survival and proliferation, we treated HRas keratinocytes with or without TGFβ1 and PERKi, or used siRNA to reduce PERK levels. Consistent with the reversal of TGFβ1-mediated IRE1α dephosphorylation and a reduced ER stress response, we observed a concomitant increase in cell survival with both PERKi treatment (Figure 4C, S6A) and siPERK (Figure S6B-D). Inhibition of PERK also significantly rescued the reduced proliferation in TGFβ1-treated HRas keratinocytes (Figure 4D, Figure S6E-H). Previous studies have also shown that TGFβ1 inhibits proliferation and accelerates senescence of HRas-expressing keratinocytes[28,31–33,37,63,64]. While TGFβ1 significantly increased the percent of SA-β-Gal positive population in both control and HRas primary keratinocytes compared to untreated controls, the percent of SA-β-Gal positive keratinocytes remained unchanged with and without PERKi (Figure S7A-C), suggesting that the decrease in proliferation is the primary response by TGFβ1 under these conditions. Together, these

results indicate that PERK-dependent dephosphorylation of IRE1α plays an important role in TGFβ1 growth inhibition of HRas-expressing keratinocytes.

To further test if IRE1α activity was required for the rescue effects of PERKi on TGFβ1-mediated growth arrest, we pre-treated keratinocytes with 20 μM 4μ8C, a small molecule inhibitor of the IRE1α RNase at a dose that inhibits the HRas-dependent increase in *Xbp1* splicing and RIDD activation (Figure S8A) and 250 nM PERKi before expressing oncogenic $HRas^{G12V}$. Inhibition of IRE1α RNase activity with 4μ8C prevented the ability of PERKi to enhance survival of TGFβ1-treated HRas keratinocytes (Figure 4C). Similarly, while 4μ8C and TGFβ1-treated HRas keratinocytes showed a higher percentage of BrdU positive population compared to its control, PERK inhibition did not significantly increase the rate of proliferation when IRE1α RNase was inactivated (Figure 4D). Furthermore, overexpressing spliced *Xbp1* mRNA in HRas keratinocytes significantly reversed the inhibition of cell viability and proliferation of TGFβ1 treated keratinocytes (Figure 4E, F, S8B). These results strongly support the requirement of PERK-mediated IRE1α dephosphorylation and inactivation as a mechanism of TGFβ1-induced growth arrest in HRas keratinocytes.

TGFβ1-induced induction of RPAP2, a PERK-dependent IRE1α phosphatase, mediates IRE1α dephosphorylation and growth inhibition in HRas keratinocytes

Inactivation of RIDD by a PERK-dependent IRE1α phosphatase, RPAP2, has been reported to disrupt the cytoprotective functions of IRE1α under irresolvable ER stress[56]. In primary keratinocytes, TGFβ1 treatment upregulated both RPAP2 protein and mRNA in HRas keratinocytes (Figure 5A, B). On the contrary, while TGFβ1 treatment upregulated RPAP2 protein in primary keratinocytes, there was no change in mRNA levels compared to the controls (Figure 5B). Moreover, primary FVB/n keratinocytes pre-treated with PERKi before exposure to increasing doses of TGFβ1 (0 – 1 ng/ml) showed a notable reduction in the levels of RPAP2 (Figure S9A), suggesting a role of PERK in RPAP2 regulation by TGFβ1. TGFβ1-dependent induction in levels of RPAP2 reduced phosphorylation at ser5 residue of RNA polymerase II subunit (POLR2A), its primary target [65] (Figure S9E). Additionally, TGFβ1-dependent induction of BiP and RPAP2 was also observed in the human HaCaT immortalized keratinocyte cell line (Figure S9B), further highlighting the role of TGFβ1 in regulating the phosphatase in keratinocytes. To demonstrate specificity of this response, we examined expression of a second IRE1α phosphatase, PP2A[66]. In both control and HRas keratinocytes, TGFβ1 downregulated the catalytic subunit (*Ppp2ca*) but its protein expression was unchanged by TGFβ1 (Figure S9C, D). At the same time, decreased mRNA expression of the regulatory subunits (*Ppp2r1a* and *Ppp2r1b*) of the phosphatase was only noted in the control keratinocytes, but not in HRas keratinocytes treated with TGFβ1 (Figure S9D). Taken together, these results demonstrate that RPAP2 is specifically induced by TGFβ1 in HRas keratinocytes.

To determine if TGFβ1-dependent activation of the PERK-RPAP2 axis plays a direct role in modulating IRE1α phosphorylation in HRas keratinocytes, we used siRNA to knockdown PERK and RPAP2 in the immortalized $HRas^{G12V}$-expressing keratinocytes. Although the immortalized cell line was less sensitive to TGFβ1-dependent IRE1α dephosphorylation compared to primary cells, depletion of PERK or RPAP2 caused a notable increase in levels

of IRE1α phosphorylation in TGFβ1-treated HRas keratinocytes (Figure 5C, Figure S10A-C). Furthermore, consistent with the increase in proliferation caused by PERK depletion, RPAP2 knockdown also caused a significant increase in the percent of proliferating keratinocytes compared to control (Figure 5D, E, S10D). RPAP2 and PERK knockdown also partially increased cyclin D1 expression in TGFβ1-treated HRas keratinocytes compared to the control (Figure 5C). These results suggest that reversal of IRE1α phosphorylation and resulting increased spliced *Xbp1* mRNA by RPAP2 or PERK knockdown (Figure 5F) prevented the reduced rate of proliferation observed in TGFβ1-treated HRas keratinocytes. Together, these results highlight a role of the PERK-RPAP2 axis to govern the IRE1α-XBP1S arm of the UPR and facilitate the tumor-suppressive functions of TGFβ1.

Discussion

TGFβ1 is a well-documented tumor-suppressor for early stages of cancer, including keratinocytes expressing oncogenic HRas and the benign tumors derived from these cells[24,25,31–34,36]. Higher demands of protein synthesis and folding induced by oncogene activation can activate all three branches of the UPR in a non-linear manner during tumorigenesis[56,67,68]. Our previous results showed that oncogenic HRas-mediated activation of the MEK-ERK pathway caused elevated IRE1α expression and activation in primary mouse keratinocytes as well as in benign and malignant cutaneous squamous tumors[26]. A growing body of literature have described role of TGFβ1 in inducing ER stress in fibrotic[40–42], inflammatory[44] and other disorders involving abnormal secretion of ECM proteins[39]. Here, we provide evidence that TGFβ1 enhances ER stress through differential modulation of the IRE1α and PERK pathways in HRas keratinocytes and this is important for TGFβ1-mediated antiproliferative effects. In keratinocytes, TGFβ1 blocked HRas-induced IRE1α phosphorylation and *Xbp1* splicing, and this occurred without a concomitant reduction in ER stress as measured by accumulation of unfolded proteins and ER expansion. TGFβ1 treatment can increase Ras activity [69]. While our results show increased HRas protein expression and a corresponding increase in phosphorylation of ERK by TGFβ1 in keratinocytes expressing mutant $HRas^{G12V}$, this increase was not associated with elevated IRE1α phosphorylation or RNase activity contrary to $HRas^{G12V}$ alone. Although our detection of IRE1α phosphorylation primarily relied on phos-tag electrophoresis, we were able to determine that phosphorylation at ser729, a critical site that can determine the overall activity of IRE1α RNase[46–48] was reduced in TGFβ1-treated HRas keratinocytes (Figure S1A). Additionally, ER stress-activated phosphorylation of ser724 was downregulated in benign papilloma expressing TGFβ1 (Figure 1D, E). These results suggest that rather than an indirect effect due to suppression of ER stress by TGFβ1, the cytokine uncouples IRE1α activation from the ER stress response while further contributing to increasing ER stress. The decrease in total BiP expression, a master regulator of ER stress[70,71], lower mRNA expression of *Xbp1s* and *Ero1-Lα,* its target that plays a key role in the disulphide bond formation of proteins synthesized in the ER[49], in TGFβ1-treated HRas keratinocytes further supports this uncoupling. Interestingly, TGFβ1-dependent dephosphorylation of IRE1α did not rescue mRNA expression of HRas-dependent RIDD targets[26], suggesting that TGFβ1 primarily affected *Xbp1* splicing in HRas keratinocytes (Figure 1B, S1D, F, G). However, we noted a significant increase in the expression of *Adamts1*, another RIDD target[26],

indicating a possible gene-specific role of TGFβ1 in these keratinocytes that necessitates further experiments (Figure S1F). At the same time, although TGFβ1 dephosphorylated IRE1α in HRas keratinocytes, it did not alter total IRE1α protein expression and suppressed ATF6 (Figure 2D). Additionally, our results show that TGFβ1 significantly increased both total and phosphorylated PERK in the keratinocytes suggesting a selective activation of this pathway. Furthermore, *BiP*, *p58*^{IPK}, *Pdia4,* and *Pdia5* mRNA expression were not downregulated by TGFβ1 suggesting that the UPR was not completely turned off under these conditions, but was only dampened through the reduction in IRE1α activity (Figure S1H, S3B).

Several reports have investigated the roles of PERK and IRE1α in regulating the UPR to control cell-fate during tumorigenesis[56,57,72]. Sustained PERK activation is primarily pro-apoptotic or cytostatic characterized either by an increase in markers of apoptosis or by a G1 arrest through cyclin D1 inhibition[54,73]. In contrast, many studies have linked the IRE1α-XBP1S axis with enhanced cell proliferation[21,26,74,75]. Our results show that both pharmacological or siRNA inhibition of PERK activation by TGFβ1 restores IRE1α phosphorylation and activity in HRas keratinocytes, indicating the importance of PERK in IRE1α dephosphorylation. Although phosphorylation at ser729 was not reversed by pharmacological inhibition of PERK (Figure S4B), we cannot rule out whether a greater PERK inhibition with GSK2606414 could have restored IRE1α phosphorylation at this site. However, a higher concentration of GSK2606414 showed off-target effects, including a notable reduction in XBP1S expression (Figure S3B) and cytotoxicity (data not shown). Furthermore, given the role of ser729 to govern RIDD activity[48] that is important to define the cell secretome[76,77], additional experiments are needed to determine if TGFβ1-PERK regulation of IRE1α phosphorylation at ser729 can suppress RIDD over time. Nonetheless, even the partial reestablishment of IRE1α activity by PERKi in TGFβ1-treated HRas keratinocytes meaningfully lowered the accumulation of unfolded proteins, as did the overexpression of human IRE1α in TGFβ1-treated HRas keratinocytes (Figure 3B, C, S4D). Our results also showed that both TGFβ1 and PERKi downregulated ATF6 expression in HRas keratinocytes suggesting that ATF6 was not driving the UPR caused by TGFβ1. Together, these results demonstrate that inactivation of IRE1α by the TGFβ1-PERK axis was necessary and sufficient to increase ER stress in these keratinocytes.

A number of IRE1α phosphatases have been identified[56,66,78–81]. Our results show that TGFβ1 upregulates expression of a PERK-dependent IRE1α phosphatase RPAP2[56] in HRas keratinocytes. In contrast to RPAP2, the mRNA expression of subunits of another IRE1α phosphatase PP2A[66], *Ppp2ca*, *Ppp2r1a* and *Ppp2r1b* were downregulated by TGFβ1, and the PP2A catalytic subunit protein expression remained unchanged (Figure S9C, D). Consistent with induction of RPAP2 levels by TGFβ1, we found a significant reduction in phosphorylation at p-ser5 of POLR2A, the primary target of RPAP2 (Figure S9E) [65]. Due to difficulties with achieving siRNA knockdown in primary keratinocytes, we utilized immortalized K5Ras keratinocytes for this study. While these keratinocytes were less sensitive to the effects of TGFβ1, siRNA-dependent silencing of RPAP2 reversed TGFβ1-dependent dephosphorylation of IRE1α. While it is possible that other reported phosphatases of IRE1α, such as Ptc2p[78], PPM1l[79], PP2Ce[80], or PTP-1B[81] may partly block or dephosphorylate IRE1α downstream of TGFβ1, our results identify a novel

TGFβ1-PERK-RPAP2 pathway that controls IRE1α phosphorylation and activation in HRas keratinocytes.

In addition to modulating the level of ER stress, the antiproliferative effects of TGFβ1 were also linked to altered activation of both PERK and IRE1α. While expression of mutant $HRas^{G12V}$ alone did not significantly modulate cell survival after 48h as determined by MTT assay, we noticed an increase in number of proliferating cells under these conditions (Figure 4A, B). The increase in BrdU positive K5Ras-T keratinocytes expressing mutant $HRas^{G12V}$ was consistent with the increased number of colonies formed after continued treatment with saturating doses of doxycycline enabling mutant $HRas^{G12V}$ expression in these cells, and this was blocked in control and mutant $HRas^{G12V}$ keratinocytes treated with 1 ng/ml TGFβ1 (Figure S5 G, H). Inhibition of PERK reversed TGFβ1-mediated growth inhibition in HRas keratinocytes, and this was dependent on restoration of IRE1α RNase function as it was prevented by the IRE1α RNase inhibitor, 4μ8c. Knockdown of RPAP2 also reversed the antiproliferative effects of TGFβ1. Moreover, PERK and RPAP2 silencing were associated to an increase in expression of spliced *Xbp1* mRNA in these keratinocytes (Figure 5F). Finally, overexpression of spliced *Xbp1* mRNA significantly attenuated the TGFβ1-induced decrease in proliferation of HRas keratinocytes. Together, these results demonstrate the importance of inhibition of the IRE1α-XBP1S axis through PERK and RPAP2 for the antiproliferative effects of TGFβ1.

Our study demonstrates a role of the UPR pathways, IRE1α and PERK in mediating cell autonomous cross-talk between TGFβ1 and HRas during the early stages of tumor development. While it is possible that altered regulation of ER-localized and secreted proteins by inactivation of RIDD may subsequently regulate TGFβ1-dependent proliferative or senescence responses under sustained ER stress caused by TGFβ1 over time, this study presents conclusive evidence that the TGFβ1-PERK-RPAP2 dependent inactivation of IRE1α and *Xbp1* splicing during the initial hyperproliferative stages of HRas-expressing keratinocytes is important for TGFβ1-mediated growth arrest. Loss of TGFβ1 signaling either due to downregulation or presence of mutations in the receptor poses an increased risk of malignant conversion and promotion[33,82,83]. While additional studies are required to investigate changes in ER stress by TGFβ1 as cells transform, our data raised the possibility that increased *Xbp1* splicing caused by inactivation of TGFβ1 signaling could be an important mechanism of malignant progression to squamous cell carcinoma.

Methods

Cell Culture

All animal studies were performed in compliance with U.S. Department of Health and Human Services Guide for the Care and Use of Laboratory Animals after the approval by The Pennsylvania State University Institutional Animal Care and Use Committee. FVB/n, C57BL/6 and the bitransgenic K5rTA x TetO-$HRas^{G12V}$ primary keratinocytes were isolated from newborn mouse epidermis and cultured in 0.05 mM Ca^{2+} EMEM (Lonza) containing 8% chelated FBS as described previously[84]. Primary double transgenic K5rTA x TetO-$HRas^{G12V}$ and C57BL/6 keratinocytes were immortalized by transduction with a lentivirus expressing SV40-T large T antigen (Addgene #12246) to generate

K5Ras-T and C57-T keratinocyte lines. STR-validated human keratinocyte HaCaT cell line (AddexBio) was cultured in 0.05 mM Ca^{2+} EMEM (Lonza) containing 8% chelated FBS. 4μ8C, 4-PBA (Cayman Chemical) GSK2606414 (PERKi) (EMD Millipore), Doxycycline (Sigma), TGFβ1 (R&D Systems), Thapsigargin (Calbiochem) were treated at indicated concentrations.

Virus production

Replication-defective high-titer retrovirus expressing v-Ras^{Ha} was generated from ψ2-producer cells as described previously[26]. Primary or immortalized mouse keratinocytes were transduced with the retrovirus in keratinocytes media containing 4 μg/ml polybrene after 3 days of culture. For lentivirus production, HEK293T cells were grown to ~60% confluence in DMEM complete media supplemented with 1 mM solidum pyruvate, 8.93 mM sodium bicarbonate, 1X NEAA, 1X GlutaMAX, and 10 mM HEPES. pCW57.1 lentiviral vector containing human wildtype IRE1α sequence was co-transfected with pMD2.G envelope (Addgene #12259) and psPAX2 packaging (Addgene #12260) vectors in a molar ratio of 2:1:1 for 6h before replacing the transfection media. pWPI-Xbp1s[26] and pLox-Ttag-iresTK (Addgene #12246) vectors were co-transfected with the pMD2.G and psPAX2 vectors in a molar ratio of 1:1:1. Lentiviral particles in the supernatant were harvested 48 and 96h post-transfection and incubated overnight with sterile 10% w/v PEG 6000 in 2.5 M NaCl at 4°C. Lentivirus was concentrated by centrifugation at 10,000 rpm for 2h at 4°C. Pellet was resuspended in sterile ice-cold PBS. Lentivirus titer was estimated by qPCR lentivirus titer kit (abm) according to manufacturer's instructions.

siRNA Transfection

K5Ras-T or C57-T cells were plated in 6-well culture trays and allowed to grow to approximately 70% confluence. Set of 4 siRNAs in a pool against RPAP2 (Horizon Cat# L-062782–01), PERK (Horizon Cat# L-044901–00) and a non-targeting control (Horizon Cat# D-001810–10) were independently transfected at a final concentration of 25 nM in serum-free, antibiotic-free EMEM media using Lipofectamine 3000 (ThermoFisher Scientific) according to the manufacturer's protocol. Transfection medium was replaced with 0.05 mM Ca^{2+}-containing EMEM keratinocytes media after 5h. Keratinocytes were cultured for an additional 4 days after transfection to allow for maximum achievable knockdown before adding doxycycline and TGFβ1 treatment for 48h. siRNA-dependent knockdown of RPAP2 and PERK was validated by qPCR and Western blot.

Confocal microscopy

Primary FVB/n keratinocytes were plated on 8-well μ-slides (IBIDI) and transduced with v-Ras^{Ha} for 2 days, followed by 1 ng/ml TGFβ1 for 48h. To measure ER content and expansion, the cells were stained with 1 μM ER-Tracker™ Green (Invitrogen) in sterile HBSS for 30 minutes at 37°C. Cells were mounted with DAPI mounting media (VectorLabs) and were visualized with LSM880 Fluorescence microscope with Airyscan (Zeiss) using the 63X oil-immersion objective. Z-stacking was performed by ImageJ. Absolute ER Area and background- and area- corrected mean fluorescence intensity were quantitated from at least 30 to 50 cells per condition using ImageJ. To measure accumulation of unfolded proteins, the keratinocytes were stained with freshly prepared 5 mM Thioflavin T (Sigma) solution

as described previously[51]. The cells were mounted with DAPI mounting media (VectorLabs) and visualized with Keyence BZ-9000 fluorescence microscope using 40X oil-immersion objective. Z-stacks were generated using ImageJ and background- and area- corrected mean fluorescence intensity was calculated from at least 30 to 50 cells per treatment condition. Statistical outliers determined by the IQR approach were removed from analysis.

Measurement of cell viability and proliferation

To measure cell survival, K5Ras-T or C57-T keratinocytes were plated in 96-well trays in quadruplets and treated with v-Ras^{Ha}/ doxycycline and TGFβ1 at indicated concentrations. Cells were pulsed with a final concentration of 0.8 μg/μl MTT (Sigma) for 3h and were lysed in 150 μl isopropanol lysis buffer (4 mM HCl, 0.1 % IGEPAL-CA630). The absorbance at 560 nm was measured using Promega GloMax multiplate reader and was normalized to untreated controls within each treatment group. To measure cell proliferation, keratinocytes were plated on 8-well μ-slides (IBIDI). 40 minutes before the indicated times, 40 μM 5-bromo-2′-deoxyuridine (BrdU) (Invitrogen) was added to the cells. The cells were then washed and fixed overnight with ice-cold 70% ethanol at −20°C. The DNA was denatured with freshly prepared 2 M HCl containing 0.5% Triton X100, followed by neutralization with 0.1 M sodium borate at pH 8.5. BrdU-labeled DNA was detected by incubation with a 1:200 anti-BrdU antibody (BD Biosciences), 1:200 biotinylated anti-mouse secondary (VectorLabs) and 1:200 Streptavidin-conjugated Alexa Fluor 488 (Invitrogen) tertiary antibodies. The DNA was stained with 1 mg/ml propidium iodide (ThermoFisher Scientific) for 10 minutes before mounting. The cells were imaged using the 10X objective on an Olympus BX43 microscope. 4 fields were imaged per condition for each experiment. BrdU positive and total cells were calculated using ImageJ automated particle counter and were expressed as a percentage of BrdU positive cells.

Statistical Analysis

All data were collected from 3 independent replicates, or at least 30 individual cells and are presented as means ± SEM. Statistical significance was determined using 2-sample t-tests with or without Welch's correction or by two-way ANOVA using GraphPad Prism v9.3.1. Tukey or Šidák post-hoc tests for multiple comparisons were performed and are specified in figure legends where applicable. Statistical significance was determined at $\alpha = 0.05$.

Generation of benign papilloma and gene constructs, Western blots, RNA extraction, qPCR, *Xbp1* splicing assay, immunostaining, colony formation assay, measurement of apoptosis and senescence are described in detail in supplementary material.

Supplementary Material

Refer to Web version on PubMed Central for supplementary material.

Acknowledgements

We thank the Huck Institutes of Life Sciences Microscopy and Flow Cytometry core facilities, and the Penn State Animal Research Program for their help. We thank Scott Oaks for providing WT hIRE1α construct. We thank Jeongin Son for his valuable input and support. This work was supported by NIH R01 CA197942, the USDA National Institute of Food and Agriculture Federal Appropriations under Project PEN04607 and 4772

and Accession number 1009993, and funding from the Department of Veterinary and Biomedical Sciences, Pennsylvania State University to AG.

Abbreviations

ATF4	Activating Transcription Factor 4
ATF6	Activating Transcription Factor 6
BiP/ Grp78	Binding immunoglobulin Protein/ Glucose regulatory protein 78
BrdU	5-bromo-2'-deoxyuridine
CHOP	CCAAT/enhancer binding protein (C/EBP) Homologous Protein
eIF2α	Eukaryotic Initiation Factor 2α
DMBA-TPA	7,12-dimethylbenz[a]anthracene - 12-O-tetradecanoylphorbol-13-acetate
ER	Endoplasmic Reticulum
ERO1-Lα	Endoplasmic Reticulum Oxidoreductase 1α
HRas	Harvey Rat Sarcoma viral oncogene homolog
IRE1α	Inositol-Requiring Enzyme 1α
PDI	Protein Disulphide Isomerase
PERK	(PKR)-like endoplasmic reticulum kinase
PP2A	Protein Phosphatase 2A
RIDD	Regulated IRE1-Dependent Decay
RPAP2	RNA Polymerase II Associated Protein 2
TGFβ1	Transforming Growth Factor β1
UPR	Unfolded Protein Response
XBP1	X-box Binding Protein 1

References

1. Chalmers F, Mogre S, Son J, Blazanin N, Glick AB. The multiple roles of the unfolded protein response regulator IRE1α in cancer. Molecular carcinogenesis. 2019;58(9):1623–1630. doi:10.1002/mc.23031 [PubMed: 31041814]
2. Hetz C, Zhang K, Kaufman RJ. Mechanisms, regulation and functions of the unfolded protein response. Nature Reviews Molecular Cell Biology. 2020/08/01 2020;21(8):421–438. doi:10.1038/s41580-020-0250-z [PubMed: 32457508]

3. Bertolotti A, Zhang Y, Hendershot LM, Harding HP, Ron D. Dynamic interaction of BiP and ER stress transducers in the unfolded-protein response. Nature Cell Biology. 2000;2(6):326–332. doi:10.1038/35014014 [PubMed: 10854322]
4. Adams CJ, Kopp MC, Larburu N, Nowak PR, Ali MMU. Structure and Molecular Mechanism of ER Stress Signaling by the Unfolded Protein Response Signal Activator IRE1. Frontiers in Molecular Biosciences. 2019;6:11. [PubMed: 30931312]
5. Ali MMU, Bagratuni T, Davenport EL, et al. Structure of the Ire1 autophosphorylation complex and implications for the unfolded protein response. The EMBO journal. 2011;30(5):894–905. doi:10.1038/emboj.2011.18 [PubMed: 21317875]
6. Yamamoto K, Sato T, Matsui T, et al. Transcriptional induction of mammalian ER quality control proteins is mediated by single or combined action of ATF6alpha and XBP1. Developmental cell. 2007;13(3):365–376. doi:10.1016/j.devcel.2007.07.018 [PubMed: 17765680]
7. Shaffer AL, Shapiro-Shelef M, Iwakoshi NN, et al. XBP1, downstream of Blimp-1, expands the secretory apparatus and other organelles, and increases protein synthesis in plasma cell differentiation. Immunity. 2004;21(1):81–93. doi:10.1016/j.immuni.2004.06.010 [PubMed: 15345222]
8. Lee A-H, Iwakoshi NN, Glimcher LH. XBP-1 regulates a subset of endoplasmic reticulum resident chaperone genes in the unfolded protein response. Molecular and cellular biology. 2003;23(21):7448–7459. doi:10.1128/MCB.23.21.7448-7459.2003 [PubMed: 14559994]
9. Pramanik J, Chen X, Kar G, et al. Genome-wide analyses reveal the IRE1a-XBP1 pathway promotes T helper cell differentiation by resolving secretory stress and accelerating proliferation. Genome Medicine. 2018/10/24 2018;10(1):76. doi:10.1186/s13073-018-0589-3 [PubMed: 30355343]
10. Park S-M, Kang T-I, So J-S. Roles of XBP1s in Transcriptional Regulation of Target Genes. Biomedicines. 2021;9(7):791. doi:10.3390/biomedicines9070791 [PubMed: 34356855]
11. Ghosh R, Wang L, Wang ES, et al. Allosteric inhibition of the IRE1α RNase preserves cell viability and function during endoplasmic reticulum stress. Cell. 2014;158(3):534–548. doi:10.1016/j.cell.2014.07.002 [PubMed: 25018104]
12. Han D, Lerner AG, Vande Walle L, et al. IRE1alpha kinase activation modes control alternate endoribonuclease outputs to determine divergent cell fates. Cell. 2009;138(3):562–575. doi:10.1016/j.cell.2009.07.017 [PubMed: 19665977]
13. Harding HP, Zhang Y, Ron D. Protein translation and folding are coupled by an endoplasmic-reticulum-resident kinase. Nature. 1999/01/01 1999;397(6716):271–274. doi:10.1038/16729 [PubMed: 9930704]
14. Rozpedek W, Pytel D, Mucha B, Leszczynska H, Diehl JA, Majsterek I. The Role of the PERK/eIF2α/ATF4/CHOP Signaling Pathway in Tumor Progression During Endoplasmic Reticulum Stress. Current molecular medicine. 2016;16(6):533–544. doi:10.2174/1566524016666160523143937 [PubMed: 27211800]
15. Ye J, Rawson RB, Komuro R, et al. ER Stress Induces Cleavage of Membrane-Bound ATF6 by the Same Proteases that Process SREBPs. Molecular Cell. 2000;6(6):1355–1364. doi:10.1016/S1097-2765(00)00133-7 [PubMed: 11163209]
16. Hillary RF, FitzGerald U. A lifetime of stress: ATF6 in development and homeostasis. Journal of Biomedical Science. 2018/05/25 2018;25(1):48. doi:10.1186/s12929-018-0453-1 [PubMed: 29801500]
17. Sheng X, Nenseth HZ, Qu S, et al. IRE1α-XBP1s pathway promotes prostate cancer by activating c-MYC signaling. Nature communications. 2019;10(1):323–323. doi:10.1038/s41467-018-08152-3
18. Tavernier Q, Legras A, Didelot A, et al. High expression of spliced X-Box Binding Protein 1 in lung tumors is associated with cancer aggressiveness and epithelial-to-mesenchymal transition. Scientific reports. 2020;10(1):10188–10188. doi:10.1038/s41598-020-67243-8 [PubMed: 32576923]
19. Lhomond S, Avril T, Dejeans N, et al. Dual IRE1 RNase functions dictate glioblastoma development. EMBO molecular medicine. 2018;10(3):e7929. doi:10.15252/emmm.201707929 [PubMed: 29311133]

20. Luo Q, Shi W, Dou B, et al. XBP1- IGFBP3 Signaling Pathway Promotes NSCLC Invasion and Metastasis. 10.3389/fonc.2021.654995. Frontiers in Oncology. 2021;11:1583.
21. Chen X, Iliopoulos D, Zhang Q, et al. XBP1 promotes triple-negative breast cancer by controlling the HIF1α pathway. Nature. 2014/04/01 2014;508(7494):103–107. doi:10.1038/nature13119 [PubMed: 24670641]
22. Sun Y, Jiang F, Pan Y, et al. XBP1 promotes tumor invasion and is associated with poor prognosis in oral squamous cell carcinoma. Oncol Rep. 2018/08/01 2018;40(2):988–998. doi:10.3892/or.2018.6498 [PubMed: 29916547]
23. Prior IA, Hood FE, Hartley JL. The Frequency of Ras Mutations in Cancer. Cancer Research. 2020;80(14):2969. doi:10.1158/0008-5472.CAN-19-3682 [PubMed: 32209560]
24. Courtois-Cox S, Jones SL, Cichowski K. Many roads lead to oncogene-induced senescence. Oncogene. 2008/05/01 2008;27(20):2801–2809. doi:10.1038/sj.onc.1210950 [PubMed: 18193093]
25. Shao J, Sheng H, DuBois RN, Beauchamp RD. Oncogenic Ras-mediated Cell Growth Arrest and Apoptosis are Associated with Increased Ubiquitin-dependent Cyclin D1 Degradation *. Journal of Biological Chemistry. 2000;275(30):22916–22924. doi:10.1074/jbc.M002235200 [PubMed: 10781597]
26. Blazanin N, Son J, Craig-Lucas AB, et al. ER stress and distinct outputs of the IRE1α RNase control proliferation and senescence in response to oncogenic Ras. Proceedings of the National Academy of Sciences of the United States of America. 2017;114(37):9900–9905. doi:10.1073/pnas.1701757114 [PubMed: 28847931]
27. Glick AB, Sporn MB, Yuspa SH. Altered regulation of TGF-beta 1 and TGF-alpha in primary keratinocytes and papillomas expressing v-Ha-ras. Molecular carcinogenesis. 1991;4(0899–1987 (Print))(3):210–219. doi:10.1002/mc.2940040308 [PubMed: 2064727]
28. Tremain R, Marko M, Kinnimulki V, Ueno H, Bottinger E, Glick A. Defects in TGFβ signaling overcome senescence of mouse keratinocytes expressing v-rasHa. Oncogene. 2000/03/01 2000;19(13):1698–1709. doi:10.1038/sj.onc.1203471 [PubMed: 10763827]
29. Massagué J. TGFbeta in Cancer. Cell. 2008;134(2):215–230. doi:10.1016/j.cell.2008.07.001 [PubMed: 18662538]
30. Inman GJ. Switching TGFβ from a tumor suppressor to a tumor promoter. Current Opinion in Genetics & Development. 2011/02/01/ 2011;21(1):93–99. doi:10.1016/j.gde.2010.12.004 [PubMed: 21251810]
31. Glick A, Popescu N, Alexander V, Ueno H, Bottinger E, Yuspa SH. Defects in transforming growth factor-β signaling cooperate with a Ras oncogene to cause rapid aneuploidy and malignant transformation of mouse keratinocytes. Proceedings of the National Academy of Sciences. 1999;96(26):14949. doi:10.1073/pnas.96.26.14949
32. Vijayachandra K, Lee J, Glick AB. Smad3 regulates senescence and malignant conversion in a mouse multistage skin carcinogenesis model. Cancer Research. 2003;63(0008–5472 (Print))(13):3447–52. [PubMed: 12839923]
33. Glick AB, Kulkarni AB, Tennenbaum T, et al. Loss of expression of transforming growth factor beta in skin and skin tumors is associated with hyperproliferation and a high risk for malignant conversion. Proceedings of the National Academy of Sciences of the United States of America. 1993;90(13):6076–6080. doi:10.1073/pnas.90.13.6076 [PubMed: 7687059]
34. Haddow S, Fowlis DJ, Parkinson K, Akhurst RJ, Balmain A. Loss of growth control by TGF-beta occurs at a late stage of mouse skin carcinogenesis and is independent of ras gene activation. Oncogene. 1991;6(0950–9232 (Print))(8):1465–1470. [PubMed: 1886717]
35. Arany PR, Rane SG, Roberts AB. Smad3 deficiency inhibits v-ras-induced transformation by suppression of JNK MAPK signaling and increased farnesyl transferase inhibition. Oncogene. 2008/04/01 2008;27(17):2507–2512. doi:10.1038/sj.onc.1210889 [PubMed: 17952112]
36. Bae D-S, Blazanin N, Licata M, Lee J, Glick AB. Tumor suppressor and oncogene actions of TGFbeta1 occur early in skin carcinogenesis and are mediated by Smad3. Molecular carcinogenesis. 2009;48(5):441–453. doi:10.1002/mc.20482 [PubMed: 18942075]
37. Liu X, Lee J, Cooley M, Bhogte E, Hartley S, Glick A. Smad7 but not Smad6 Cooperates with Oncogenic ras to Cause Malignant Conversion in a Mouse Model for Squamous Cell Carcinoma. Cancer Research. 2003;63(22):7760. [PubMed: 14633701]

38. Markell LM, Masiuk KE, Blazanin N, Glick AB. Pharmacologic inhibition of ALK5 causes selective induction of terminal differentiation in mouse keratinocytes expressing oncogenic HRAS. Molecular cancer research: MCR. 2011;9(6):746–756. doi:10.1158/1541-7786.MCR-11-0112 [PubMed: 21521744]
39. Okumura N, Hashimoto K, Kitahara M, et al. Activation of TGF-β signaling induces cell death via the unfolded protein response in Fuchs endothelial corneal dystrophy. Scientific Reports. 2017/07/28 2017;7(1):6801. doi:10.1038/s41598-017-06924-3 [PubMed: 28754918]
40. Lenna S, Trojanowska M. The role of endoplasmic reticulum stress and the unfolded protein response in fibrosis. Current opinion in rheumatology. 2012;24(6):663–668. doi:10.1097/BOR.0b013e3283588dbb [PubMed: 22918530]
41. Kropski JA, Blackwell TS. Endoplasmic reticulum stress in the pathogenesis of fibrotic disease. The Journal of Clinical Investigation. 01/02/ 2018;128(1):64–73. doi:10.1172/JCI93560 [PubMed: 29293089]
42. Stauffer WT, Blackwood EA, Azizi K, Kaufman RJ, Glembotski CC. The ER Unfolded Protein Response Effector, ATF6, Reduces Cardiac Fibrosis and Decreases Activation of Cardiac Fibroblasts. International journal of molecular sciences. 2020;21(4):1373. doi:10.3390/ijms21041373
43. Baek HA, Kim DS, Park HS, et al. Involvement of Endoplasmic Reticulum Stress in Myofibroblastic Differentiation of Lung Fibroblasts. American Journal of Respiratory Cell and Molecular Biology. 2012/06/01 2012;46(6):731–739. doi:10.1165/rcmb.2011-0121OC [PubMed: 21852685]
44. Huang H, Ding Q-l, Zhu H-f, Yang D-f. Roles of TGF-β signaling pathway in endoplasmic reticulum stress in endothelial cells stimulated with cigarette smoke extract. Current Medical Science. 2017/10/01 2017;37(5):699–704. doi:10.1007/s11596-017-1791-z
45. Huang Y, Liu J, Fan L, et al. miR-663 overexpression induced by endoplasmic reticulum stress modulates hepatocellular carcinoma cell apoptosis via transforming growth factor beta 1. OncoTargets and therapy. 2016;9:1623–1633. doi:10.2147/OTT.S96902 [PubMed: 27073326]
46. Prischi F, Nowak PR, Carrara M, Ali MMU. Phosphoregulation of Ire1 RNase splicing activity. Nature Communications. 2014;5(1):3554. doi:10.1038/ncomms4554
47. Ferri E, Le Thomas A, Wallweber HA, et al. Activation of the IRE1 RNase through remodeling of the kinase front pocket by ATP-competitive ligands. Nature communications. 2020;11(1):6387–6387. doi:10.1038/s41467-020-19974-5
48. Tang C- HA, Chang S, Paton AW, et al. Phosphorylation of IRE1 at S729 regulates RIDD in B cells and antibody production after immunization. The Journal of cell biology. 2018;217(5):1739–1755. doi:10.1083/jcb.201709137 [PubMed: 29511123]
49. Cabibbo A, Pagani M, Fabbri M, et al. ERO1-L, a Human Protein That Favors Disulfide Bond Formation in the Endoplasmic Reticulum*. Journal of Biological Chemistry. 2000/02/18/2000;275(7):4827–4833. doi:10.1074/jbc.275.7.4827 [PubMed: 10671517]
50. Mohammed J, Ryscavage A, Perez-Lorenzo R, Gunderson AJ, Blazanin N, Glick AB. TGFβ1-Induced Inflammation in Premalignant Epidermal Squamous Lesions Requires IL-17. Journal of Investigative Dermatology. 2010;130(9):2295–2303. doi:10.1038/jid.2010.92 [PubMed: 20410912]
51. Beriault DR, Werstuck GH. Detection and quantification of endoplasmic reticulum stress in living cells using the fluorescent compound, Thioflavin T. Biochimica et Biophysica Acta (BBA) - Molecular Cell Research. 2013;1833(10):2293–2301. [PubMed: 23747341]
52. Rellmann Y, Gronau I, Hansen U, Dreier R. 4-Phenylbutyric Acid Reduces Endoplasmic Reticulum Stress in Chondrocytes That Is Caused by Loss of the Protein Disulfide Isomerase ERp57. Oxidative Medicine and Cellular Longevity. 2019/10/29 2019;2019:6404035. doi:10.1155/2019/6404035 [PubMed: 31781343]
53. Kranz P, Sänger C, Wolf A, et al. Tumor cells rely on the thiol oxidoreductase PDI for PERK signaling in order to survive ER stress. Scientific Reports. 2020/09/17 2020;10(1):15299. doi:10.1038/s41598-020-72259-1 [PubMed: 32943707]

54. Gonen N, Sabath N, Burge CB, Shalgi R. Widespread PERK-dependent repression of ER targets in response to ER stress. Scientific Reports. 2019/03/13 2019;9(1):4330. doi:10.1038/s41598-019-38705-5 [PubMed: 30867432]
55. Teske BF, Wek SA, Bunpo P, et al. The eIF2 kinase PERK and the integrated stress response facilitate activation of ATF6 during endoplasmic reticulum stress. Molecular Biology of the Cell. 2011/11/15 2011;22(22):4390–4405. doi:10.1091/mbc.e11-06-0510 [PubMed: 21917591]
56. Chang T-K, Lawrence DA, Lu M, et al. Coordination between Two Branches of the Unfolded Protein Response Determines Apoptotic Cell Fate. Molecular Cell. 2018;71(4):629–636.e5. [PubMed: 30118681]
57. Gupta A, Hossain MM, Read DE, Hetz C, Samali A, Gupta S. PERK regulated miR-424(322)-503 cluster fine-tunes activation of IRE1 and ATF6 during Unfolded Protein Response. Scientific Reports. 2015/12/17 2015;5(1):18304. doi:10.1038/srep18304 [PubMed: 26674075]
58. Lou Z, Gong YQ, Zhou X, Hu GH. Low expression of miR−199 in hepatocellular carcinoma contributes to tumor cell hyper−proliferation by negatively suppressing XBP1. Oncol Lett. 2018/11/01 2018;16(5):6531–6539. doi:10.3892/ol.2018.9476 [PubMed: 30405792]
59. Maurel M, Chevet E, Tavernier J, Gerlo S. Getting RIDD of RNA: IRE1 in cell fate regulation. Trends in Biochemical Sciences. 2014;39(5):245–254. doi:10.1016/j.tibs.2014.02.008 [PubMed: 24657016]
60. Kadowaki H, Nishitoh H, Ichijo H. Survival and apoptosis signals in ER stress: the role of protein kinases. Journal of Chemical Neuroanatomy. 2004/09/01/ 2004;28(1):93–100. doi:10.1016/j.jchemneu.2004.05.004 [PubMed: 15363494]
61. Spencer BG, Finnie JW. The Role of Endoplasmic Reticulum Stress in Cell Survival and Death. Journal of Comparative Pathology. 2020/11/01/ 2020;181:86–91. doi:10.1016/j.jcpa.2020.10.006 [PubMed: 33288157]
62. Corazzari M, Gagliardi M, Fimia GM, Piacentini M. Endoplasmic Reticulum Stress, Unfolded Protein Response, and Cancer Cell Fate. 10.3389/fonc.2017.00078. Frontiers in Oncology. 2017;7:78. [PubMed: 28491820]
63. Ueda S, Tominaga T, Ochi A, et al. TGF-β1 is involved in senescence-related pathways in glomerular endothelial cells via p16 translocation and p21 induction. Scientific Reports. 2021/11/04 2021;11(1):21643. doi:10.1038/s41598-021-01150-4 [PubMed: 34737348]
64. Vijayachandra K, Higgins W, Lee J, Glick A. Vijayachandra K, Higgins W, Lee J, Glick A. Induction of p16ink4a and p19ARF by TGFbeta1 contributes to growth arrest and senescence response in mouse keratinocytes. Mol Carcinog 48: 181–186. Molecular carcinogenesis. 03/01 2009;48:181–6. doi:10.1002/mc.20472 [PubMed: 18655107]
65. Egloff S, Zaborowska J, Laitem C, Kiss T, Murphy S. Ser7 phosphorylation of the CTD recruits the RPAP2 Ser5 phosphatase to snRNA genes. Molecular cell. 2012;45(1):111–122. doi:10.1016/j.molcel.2011.11.006 [PubMed: 22137580]
66. Qiu Y, Mao T, Zhang Y, et al. A Crucial Role for RACK1 in the Regulation of Glucose-Stimulated IRE1α Activation in Pancreatic β Cells. Science Signaling. 2010;3(106):ra7. doi:10.1126/scisignal.2000514 [PubMed: 20103773]
67. Wang M, Kaufman RJ. The impact of the endoplasmic reticulum protein-folding environment on cancer development. Nature Reviews Cancer. 2014/09/01 2014;14(9):581–597. doi:10.1038/nrc3800 [PubMed: 25145482]
68. Urra H, Dufey E, Avril T, Chevet E, Hetz C. Endoplasmic Reticulum Stress and the Hallmarks of Cancer. Review. Trends in Cancer. May 2016;2(5):252–262. doi:10.1016/j.trecan.2016.03.007 [PubMed: 28741511]
69. Grusch M, Petz M, Metzner T, Oztürk D, Schneller D, Mikulits W. The crosstalk of RAS with the TGF-β family during carcinoma progression and its implications for targeted cancer therapy. Current cancer drug targets. 2010;10(8):849–857. doi:10.2174/156800910793357943 [PubMed: 20718708]
70. Pobre KFR, Poet GJ, Hendershot LM. The endoplasmic reticulum (ER) chaperone BiP is a master regulator of ER functions: Getting by with a little help from ERdj friends. Journal of Biological Chemistry. 2019;294(6):2098–2108. doi:10.1074/jbc.REV118.002804 [PubMed: 30563838]

71. Lee AS. The ER chaperone and signaling regulator GRP78/BiP as a monitor of endoplasmic reticulum stress. Methods. 2005/04/01/ 2005;35(4):373–381. doi:10.1016/j.ymeth.2004.10.010 [PubMed: 15804610]
72. Lin JH, Li H, Zhang Y, Ron D, Walter P. Divergent Effects of PERK and IRE1 Signaling on Cell Viability. PLOS ONE. 2009;4(1):e4170. doi:10.1371/journal.pone.0004170 [PubMed: 19137072]
73. Brewer JW, Diehl JA. PERK mediates cell-cycle exit during the mammalian unfolded protein response. Proceedings of the National Academy of Sciences. 2000;97(23):12625. doi:10.1073/pnas.220247197
74. Thorpe JA, Schwarze SR. IRE1α controls cyclin A1 expression and promotes cell proliferation through XBP-1. Cell Stress and Chaperones. 2010/09/01 2010;15(5):497–508. doi:10.1007/s12192-009-0163-4 [PubMed: 20013084]
75. Zhang K, Liu H, Song Z, et al. The UPR Transducer IRE1 Promotes Breast Cancer Malignancy by Degrading Tumor Suppressor microRNAs. iScience. 2020/09/25/ 2020;23(9):101503. doi:10.1016/j.isci.2020.101503
76. Logue SE, McGrath EP, Cleary P, et al. Inhibition of IRE1 RNase activity modulates the tumor cell secretome and enhances response to chemotherapy. Nature Communications. 2018;9(1):3267. doi:10.1038/s41467-018-05763-8
77. Dejeans N, Pluquet O, Lhomond S, et al. Autocrine control of glioma cells adhesion and migration through IRE1α-mediated cleavage of SPARC mRNA. Journal of Cell Science. 2012;125(18):4278. doi:10.1242/jcs.099291 [PubMed: 22718352]
78. Welihinda AA, Tirasophon W, Green SR, Kaufman RJ. Protein serine/threonine phosphatase Ptc2p negatively regulates the unfolded-protein response by dephosphorylating Ire1p kinase. Molecular and cellular biology. 1998;18(4):1967–1977. doi:10.1128/MCB.18.4.1967 [PubMed: 9528768]
79. Lu G, Ota A, Ren S, et al. PPM1l encodes an inositol requiring-protein 1 (IRE1) specific phosphatase that regulates the functional outcome of the ER stress response. Molecular metabolism. 2013;2(4):405–416. doi:10.1016/j.molmet.2013.07.005 [PubMed: 24327956]
80. Ren S, Lu G, Ota A, et al. IRE1 Phosphatase PP2Ce Regulates Adaptive ER Stress Response in the Postpartum Mammary Gland. PLOS ONE. 2014;9(11):e111606. doi:10.1371/journal.pone.0111606
81. Gu F, Nguyên DT, Stuible M, Dubé N, Tremblay ML, Chevet E. Protein-tyrosine Phosphatase 1B Potentiates IRE1 Signaling during Endoplasmic Reticulum Stress *. Journal of Biological Chemistry. 2004;279(48):49689–49693. doi:10.1074/jbc.C400261200 [PubMed: 15465829]
82. Guasch G, Schober M, Pasolli HA, Conn EB, Polak L, Fuchs E. Loss of TGFbeta signaling destabilizes homeostasis and promotes squamous cell carcinomas in stratified epithelia. Cancer cell. 2007;12(4):313–327. doi:10.1016/j.ccr.2007.08.020 [PubMed: 17936557]
83. Rose AM, Sansom OJ, Inman GJ. Loss of TGF-β signaling drives cSCC from skin stem cells – More evidence. Cell Cycle. 2017/03/04 2017;16(5):386–387. doi:10.1080/15384101.2016.1259892 [PubMed: 27860538]
84. Lichti U, Anders J, Yuspa SH. Isolation and short-term culture of primary keratinocytes, hair follicle populations and dermal cells from newborn mice and keratinocytes from adult mice for in vitro analysis and for grafting to immunodeficient mice. Nature protocols. 2008;3(5):799–810. doi:10.1038/nprot.2008.50 [PubMed: 18451788]

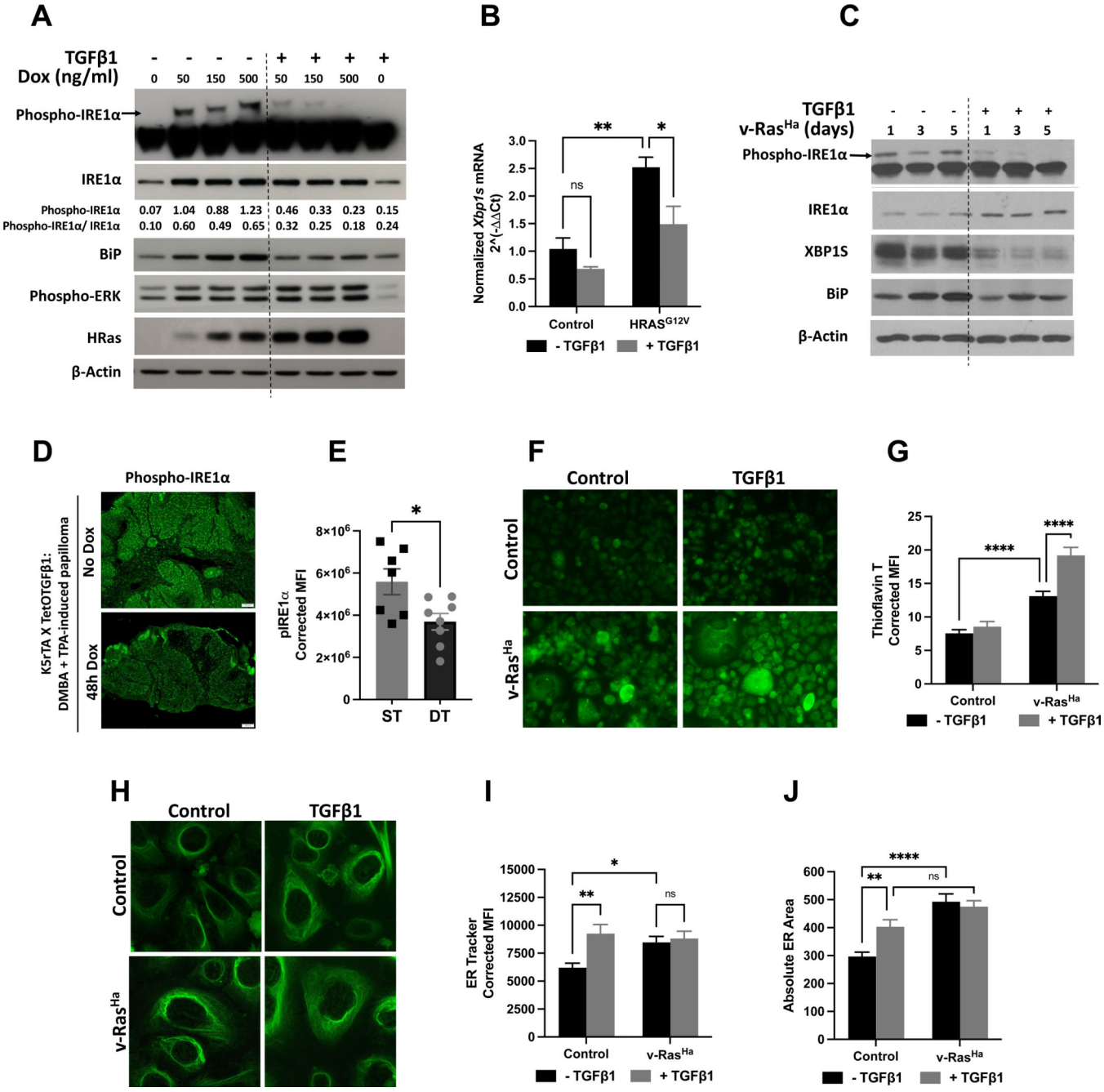

Figure 1: TGFβ1 blocks HRas-induced IRE1α phosphorylation without a corresponding reduction in ER stress.

(A) Phos-tag Western blot for phospho-IRE1α and Western blot analysis of total IRE1α, BiP, Phospho-ERK, and HRas in K5Ras^{G12V} primary keratinocytes treated simultaneously with increasing doses (0 – 500 ng/ml) of doxycycline and 1 ng/ml TGFβ1 for 48h. Numbers represent phospho- and total IRE1α densitometry normalized to β-actin. (B) qPCR analysis showing spliced *Xbp1* mRNA expression 48h after addition of 1 ng/ml TGFβ1 to K5Ras^{G12V} primary keratinocytes treated with 500 ng/ml doxycycline. (C) Phos-tag Western blot for phospho-IRE1α and Western blot analysis of total IRE1α, XBP1S, and BiP in

C57BL/6 primary keratinocytes expressing v-Ras^{Ha} and treated with 1 ng/ml TGFβ1 for 1, 3, and 5 days. (D) Representative immunofluorescence images and (E) area-corrected mean fluorescence intensity (MFI) for phospho-ser724-IRE1α in DMBA-TPA-induced benign papilloma with and without overexpression of TGFβ1 for 48h. Scale bar is 100 μm. Statistical significance was determined by t-test using Welch's correction. (F) Representative fluorescence confocal images and (G) area-corrected mean fluorescence intensity (MFI) of thioflavin-T-stained C57-T keratinocytes expressing v-Ras^{Ha} and treated with 1 ng/ml TGFβ1 for 48h. Scale bar is 25 μm. (H) Representative fluorescence confocal images, (I) area-corrected mean fluorescence intensity (MFI), and (J) ER area of primary FVB/n keratinocytes expressing v-Ras^{Ha} and treated with 1 ng/ml TGFβ1 for 48h and stained with ER Tracker™ Green. Scale bar is 20 μm. Data represent mean ± SEM from 3 biological replicates, or at least 50 cells per condition. Statistical significance was determined by two-way ANOVA and Tukey post-hoc test for multiple comparisons at $p < 0.05$.

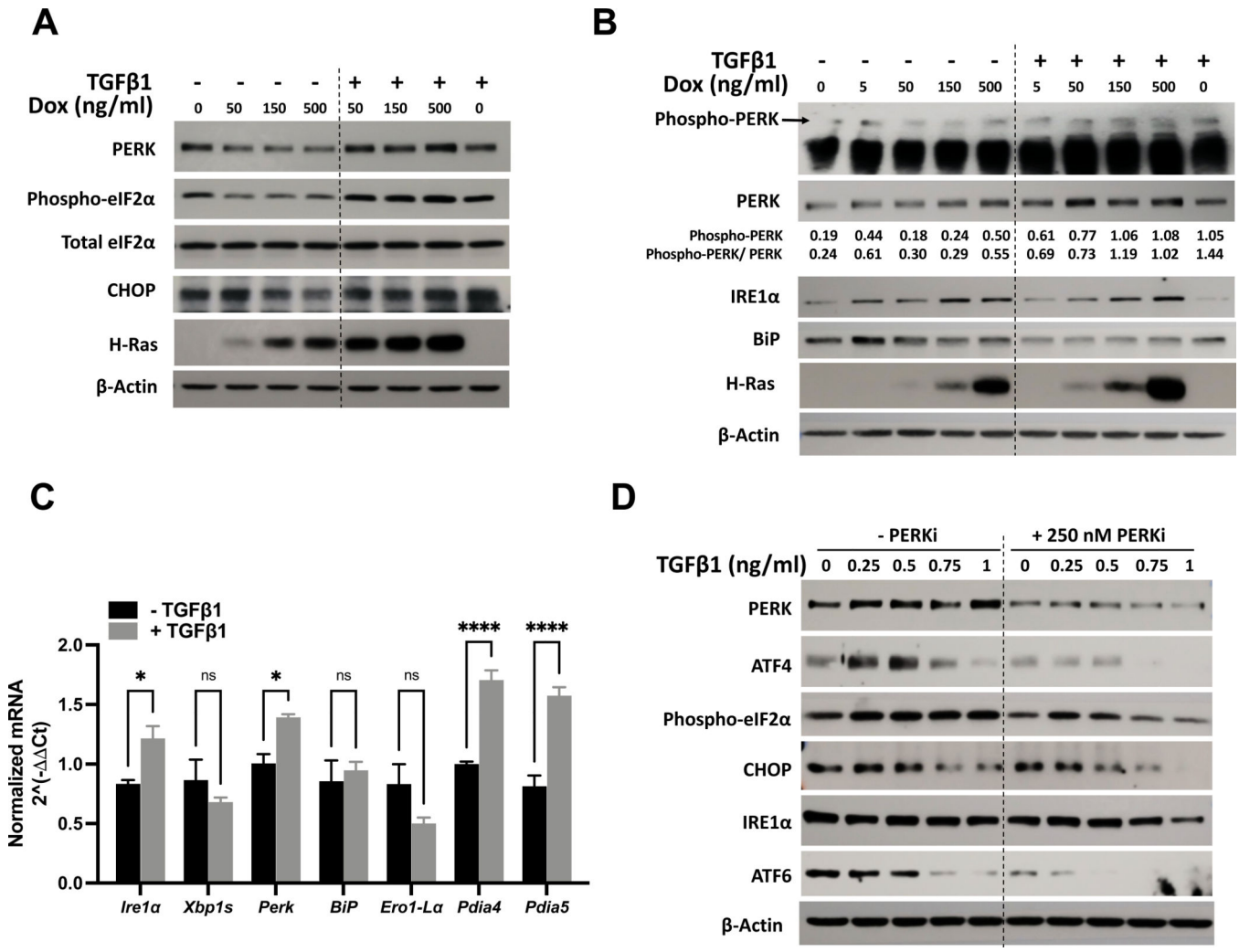

Figure 2: TGFβ1 activates PERK signaling.

(A) Western blot analysis of PERK, phospho- and total eIF2α, CHOP, and HRas in K5Ras^{G12V} primary keratinocytes treated simultaneously with increasing doses (0 – 500 ng/ml) of doxycycline and 1 ng/ml TGFβ1 for 48h. (B) Phos-tag Western blot for phospho-PERK and Western blot analysis of total PERK, IRE1α, BiP, and HRas in K5Ras-T keratinocytes treated with 0 – 500 ng/ml doxycycline with and without 1 ng/ml TGFβ1 for 48h. Numbers represent phospho- and total PERK densitometry normalized to β-actin. (C) qPCR analysis of ER stress markers in primary K5Ras^{G12V} keratinocytes treated with 1 ng/ml TGFβ1 for 48h. Statistical significance was determined by Student's t-test at $p < 0.05$. (D) Western blot of PERK, ATF4, phospho-eIF2α, CHOP, IRE1α, and ATF6 in K5Ras-T cells pre-treated with 250 nM PERK inhibitor (PERKi) and increasing doses (0 – 1 ng/ml) of TGFβ1 for 48h.

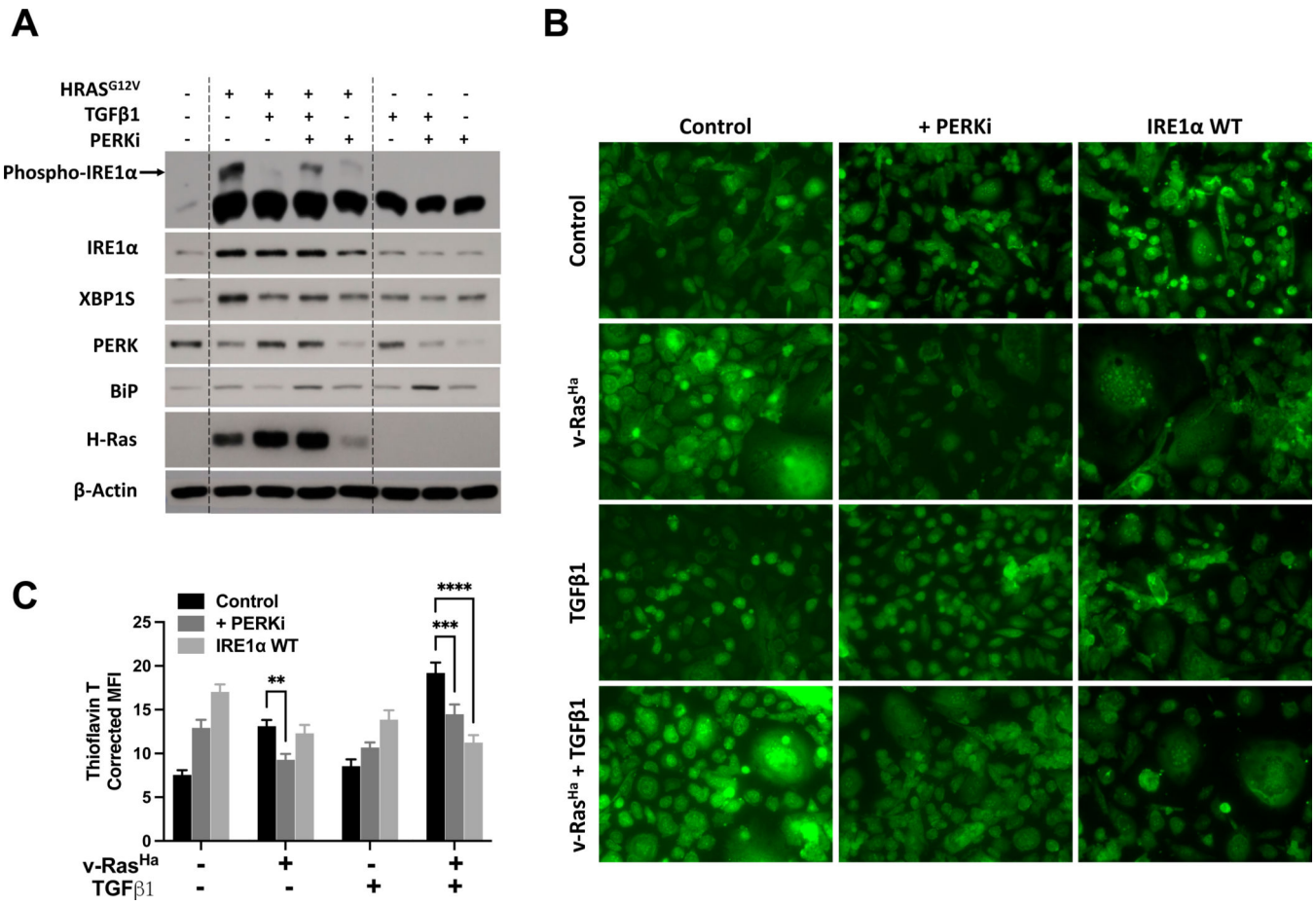

Figure 3: Inhibition of PERK signaling partially rescued TGFβ1-dependent IRE1α dephosphorylation and accumulation of unfolded proteins in HRas keratinocytes.

(A) Phos- tag Western blot for phospho-IRE1α and Western blot analysis of total IRE1α, XBP1S, PERK, BiP, and HRas in K5Ras^{G12V} primary keratinocytes treated simultaneously with 500 ng/ml doxycycline and 1 ng/ml TGFβ1 for 48h. Keratinocytes were pre-treated with 250 nM PERK inhibitor (PERKi) for 1h where indicated before the addition of doxycycline and TGFβ1. (B) Representative fluorescence confocal images and (C) area-corrected mean fluorescence intensity (MFI) of thioflavin-T-stained C57-T keratinocytes expressing v-Ras^{Ha} and treated with 1 ng/ml TGFβ1. Keratinocytes were pre-treated with 250 nM PERKi for 1h where indicated. Overexpression of wildtype human IRE1α (IRE1α WT) was induced with 500 ng/ml doxycycline for 24h before treatment with 1 ng/ml of TGFβ1 for additional 48h. Data represent mean ± SEM for at least 30 cells. Scale bar is 25 μm. Statistical significance was determined by two-way ANOVA and Tukey post-hoc test for multiple comparisons at $p < 0.05$.

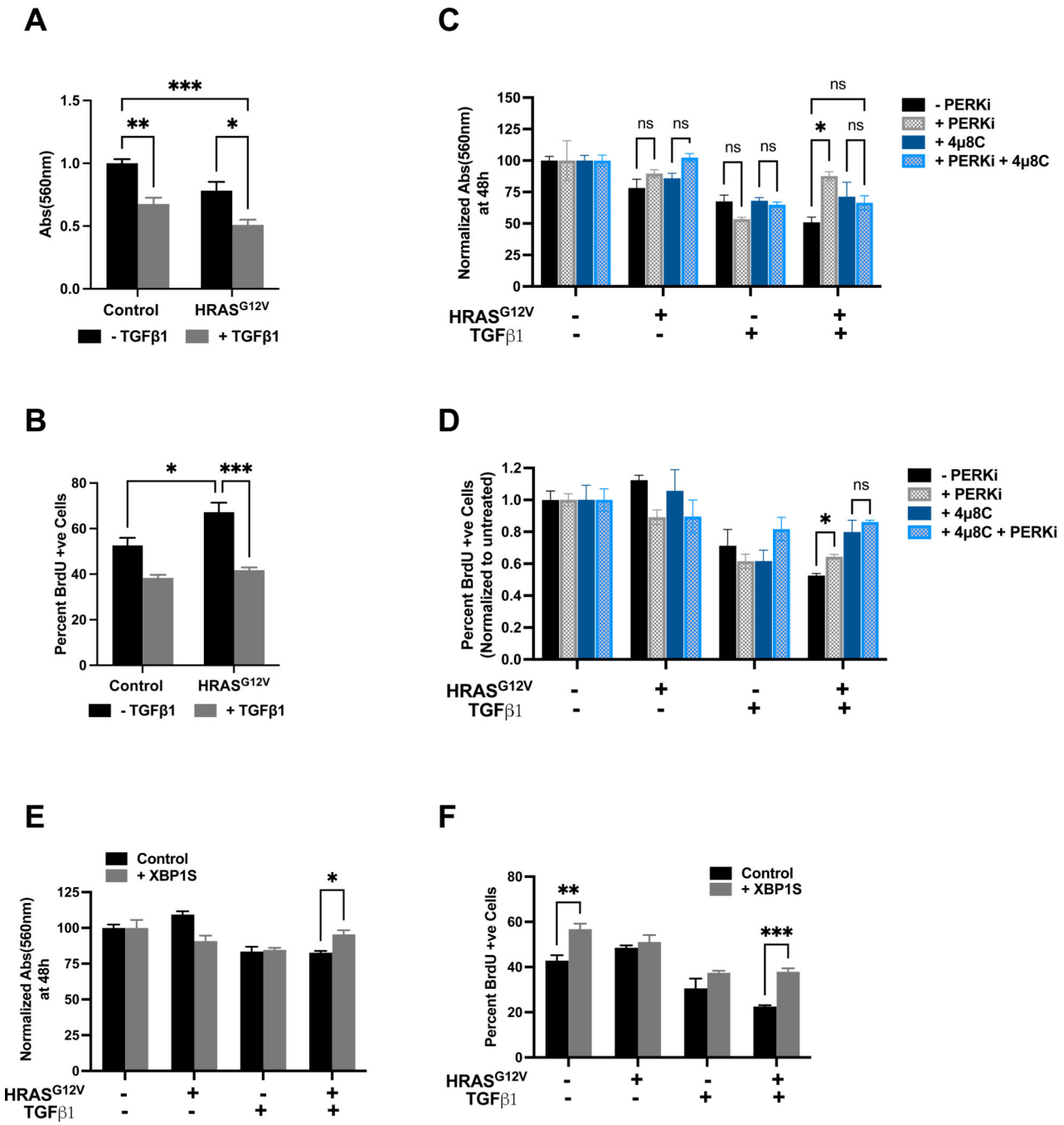

Figure 4: TGFβ1-PERK-dependent dephosphorylation of IRE1α in HRas keratinocytes regulates cell proliferation.

(A) MTT absorbance at 560 nm and (B) percent BrdU positive K5Ras-T keratinocytes treated simultaneously with 500 ng/ml doxycycline and 1 ng/ml TGFβ1 for 48h. (C) Normalized MTT absorbance at 560 nm and (D) percent BrdU positive K5Ras-T keratinocytes pre-treated with 250 nM PERKi for 1h or 20 μM 4μ8C for 24h, followed by 500 ng/ml doxycycline and 1 ng/ml TGFβ1 for 48h. Data were normalized to controls within each treatment group. Data represent mean ± SEM from 3 biological replicates. Statistical significance was determined by two-way ANOVA and Tukey post-hoc test

for multiple comparisons at $p < 0.05$. (E) Normalized MTT absorbance at 560 nm and (F) Percent BrdU positive K5Ras-T keratinocytes overexpressing spliced *Xbp1* mRNA treated simultaneously with 500 ng/ml doxycycline and 1 ng/ml TGFβ1 for 48h. Statistical significance was determined by two-way ANOVA and Šidák post-hoc test for multiple comparisons at $p < 0.05$.

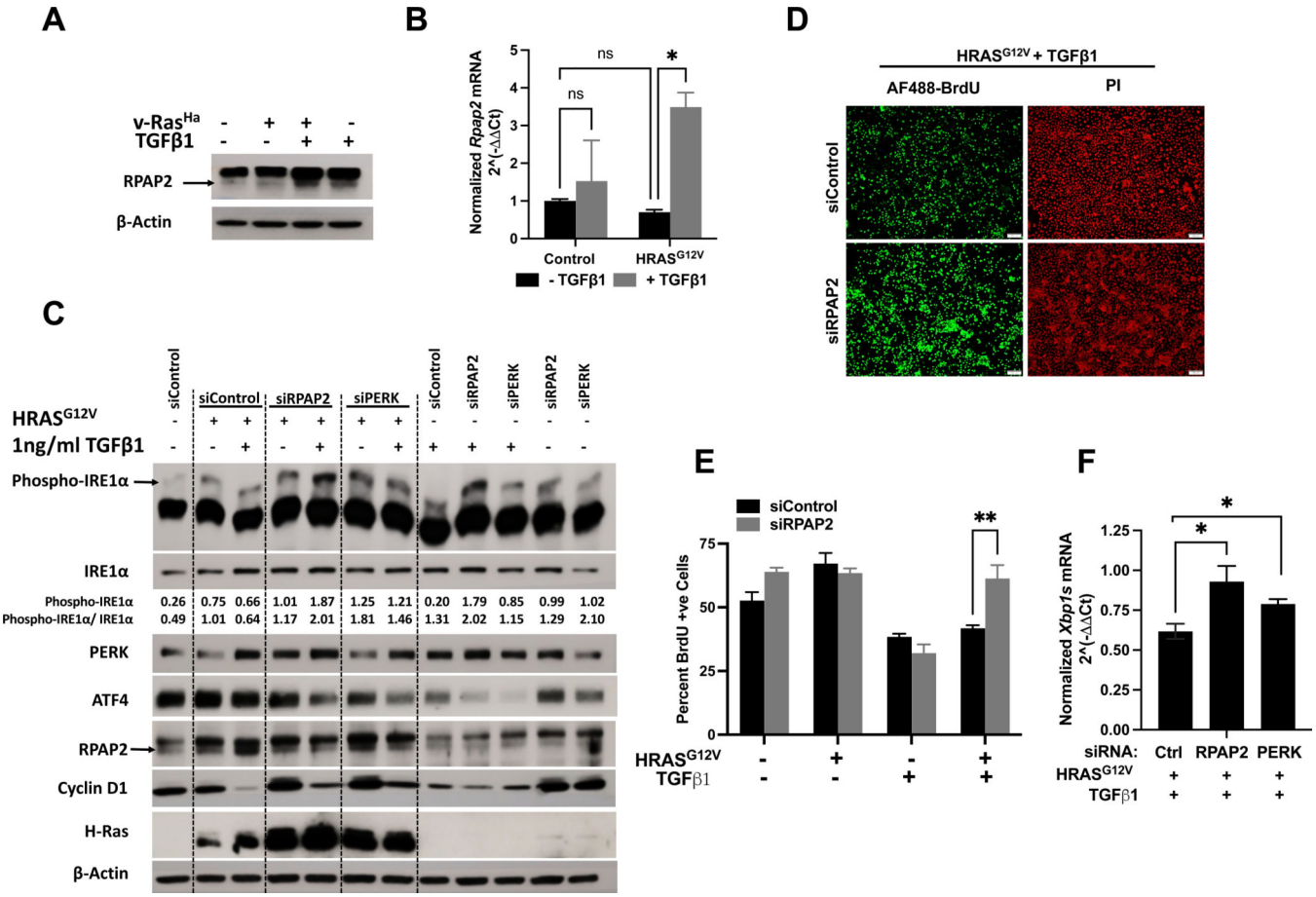

Figure 5: TGFβ1-PERK-RPAP2 axis governs IRE1α activity in HRas keratinocytes.

(A) Western blot of RPAP2 expression in FVB/n primary keratinocytes expressing v-Ras^{Ha} and treated with 1 ng/ml TGFβ1 for 48h. (B) qPCR analysis of K5Ras^{G12V} primary keratinocytes treated simultaneously with 500 ng/ml doxycycline and 1 ng/ml TGFβ1 for 48h. Data represent mean ± SEM from 3 biological replicates. Statistical significance was determined by two-way ANOVA and Tukey post-hoc test for multiple comparisons at $p < 0.05$. (C) Phos-tag Western blot for phospho-IRE1α and Western blot of total IRE1α, PERK, ATF4, RPAP2, Cyclin D1, and HRas in RPAP2 and PERK-depleted K5Ras-T keratinocytes. Keratinocytes were treated with 500 ng/ml doxycycline and 1 ng/ml TGFβ1 4 days after transfection of siRNAs against RPAP2 and PERK. Numbers represent phospho- and total IRE1α densitometry normalized to β-actin. (D) Representative fluorescence images of AF488-BrdU (green) and propidium iodide (PI) (red) and (E) percent BrdU positive control and RPAP2 knockdown K5Ras-T keratinocytes. Scale bar is 100 μm. Data represent mean ± SEM from 3 biological replicates. Statistical significance was determined by two-way ANOVA and Šidák post-hoc test for multiple comparisons at $p < 0.05$. (F) qPCR analysis showing spliced *Xbp1* mRNA expression in K5Ras-T RPAP2 and PERK knockdown keratinocytes treated with 500 ng/ml doxycycline and 1 ng/ml TGFβ1 for 48h. Data represent mean ± SEM from 3 biological replicates. Statistical significance was determined by Student's t-test at $p < 0.05$.

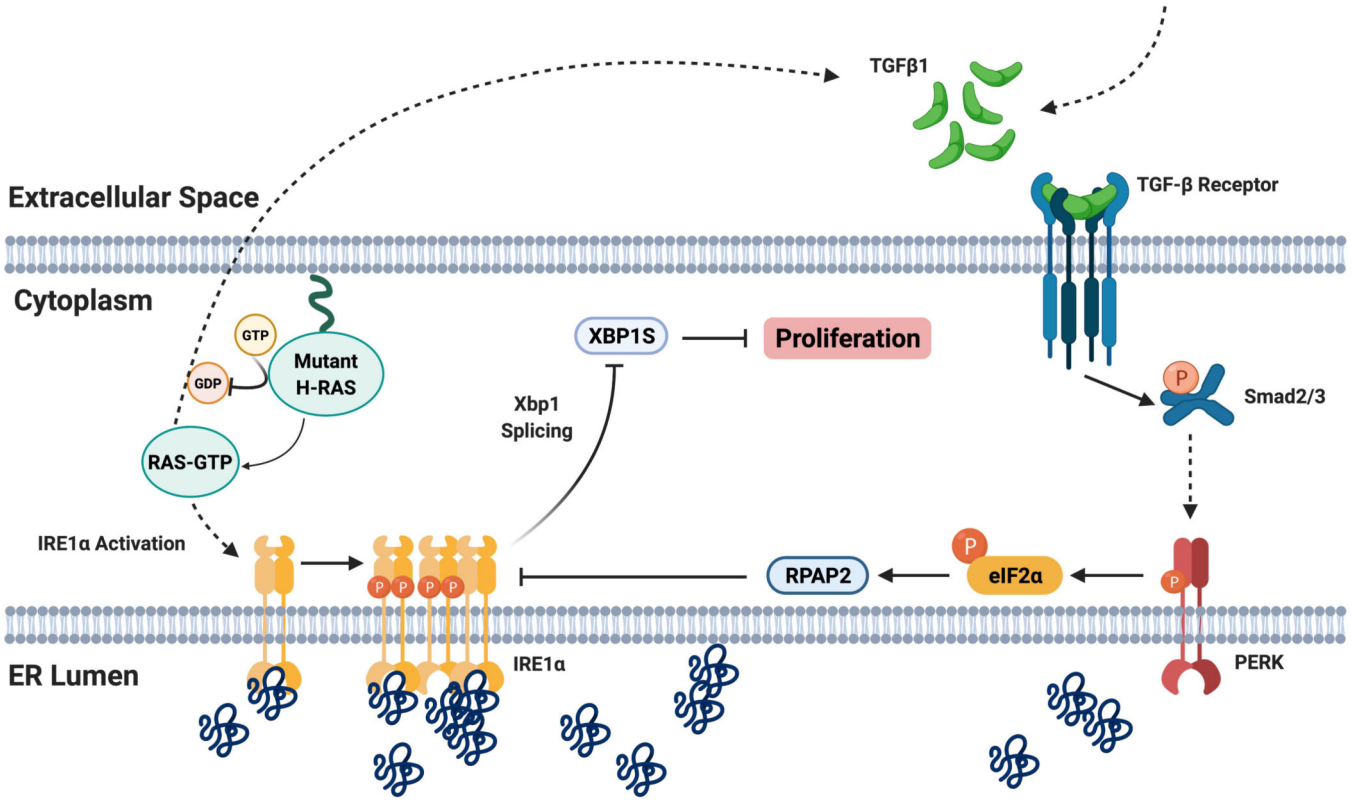

Figure 6: Proposed model of TGFβ1-regulation of IRE1α phosphorylation in oncogenic HRas keratinocytes.

TGFβ1 suppresses HRas-induced IRE1α phosphorylation and activation in mouse keratinocytes resulting in reduced *Xbp1* splicing and XBP1S protein notwithstanding the increasing accumulation of unfolded protein in the ER lumen. This uncoupling of ER stress and IRE1α activation is mediated by TGFβ1-PERK signaling. PERK activation by TGFβ1 specifically upregulates an IRE1α phosphatase, RPAP2. The decrease in *Xbp1* splicing by TGFβ1-PERK-RPAP2 contributes to the significantly lower proliferation of HRas keratinocytes. Created with BioRender.com.